Analysis of Composite Scattering from a Target Above/Below a Dielectric Rough Surface using Higher Order Basis Functions

Yuyuan An [1], Rushan Chen [1], Pingping Xu [1], Zhiwei Liu [2], and Liping Zha [1]

[1] Department of Communication Engineering
Nanjing University of Science and Technology, Nanjing, 210094, China
ayy.2@163.com, eerschen@njust.edu.cn, xupingping921@126.com, daisy918@163.com

[2] School of Information Engineering
East China Jiaotong University, Nanchang, 330013, China
zwliu1982@hotmail.com

Abstract ─ In this paper, the validity of four types of higher order basis functions for analyzing the 3D EM scattering from the target and dielectric rough surface is investigated. Although the higher order basis functions can reduce the number of unknowns significantly, the iterative solution time may increase with the order of the basis because the matrix condition numbers deteriorates with the basis order increase. This may be relative to: (a) The truncation of the dielectric rough surface and the interaction between the object and the rough surface; (b) the properties of the basis functions adopted. In this paper, a variety of models including a rough surface only, an object above or below the rough surface are investigated with different higher order basis functions. The program is based on the Poggio-Miller-Chang-Harrington-Wu-Tsai (PMCHW) integral equations. The multilevel fast multipole algorithm (MLFMA) and flexible generalized minimal residual (FGMRES) techniques are used to further accelerate the iteration solution.

Index Terms ─ Electromagnetic scattering, higher order basis functions, MLFMA, rough surface.

I. INTRODUCTION

Electromagnetic scattering from dielectric rough surfaces has a large number of applications, such as remote sensing, radar surveillance, and ground-penetration radar probing [1-9, 29]. Specific examples include detection of landmines and remote sensing of soil moisture content to retrieve snow depth. Numerical simulation of the combined target and rough surface model is complicated by the interactions between the target and the rough surface background [1]. During the past few decades, both the approximate and rigorous methods have been developed to tackle this problem. Among the approximate methods, some are based on small perturbation method (SPM) [10], Kirchhoff approximation (KA) [3], small slope approximation (SSA) [11] and so on. However, the height value must be very small compared to the electromagnetic wave length in the SPM; the radius of the surface must be larger than a wavelength in the KA; the slope must be small and the height must be moderate for the first order in the SSA.

Numerical solution, on the other hand, is a rigorous approach which can deal with most of the cases without considering the profile of the rough surfaces. For the 2D problems, the generalized forward backward method with spectral acceleration algorithm (GFBM/SAA) [12], the finite element method (FEM) [13], the extended boundary condition method (EBCM) [33], and the steepest descent-fast multipole algorithm have been successfully used to the target and rough surface composite model. However, scattering from a 3D target and rough surface composite model is much more complicated than in a 2D case because of the large computational complexity [4]. Till now, only very few reports have been found for the 3D case, e.g. the UV

Submitted On: Feb. 13, 2012
Accepted On: April 25, 2012

method [4], the FDTD method [14, 30], and the steepest descent-fast multipole method (SDFMM) [2,6].

In order to reduce the computational complexity, some efficient algorithms have been developed. The sparse matrix flat surface iterative approach (SMFSIA) [15, 16] takes advantage of the fact that rough surfaces are "nearly" planar. In this approach, the Green's function for the weak matrix elements has been expanded in a Taylor's series about the flat surface, which maps the problem to a flat 2D surface. The FFT technique is then used to accelerate the matrix-vector product for the Toeplitz structure of the interaction matrix on the flat surface. The complexity of the SMFSIA is $O(N \log N)$. Another approach is SDFMM [31], which has expressed the free-space dyadic Green's function in terms of a rapidly converging Sommerfeld steepest descent integral. The source and observation points are evaluated efficiently by using a multilevel FMM-like algorithm based on inhomogeneous plane wave expansion. The time and memory complexity are $O(N)$.

There is still an efficient approach that is based on the consideration of basis functions [7] [17-18, 34-38]. For example, the characteristic basis function method (CBFM) [7] proposed for electromagnetic scattering over rough terrain profiles, is based on the constructing of high-level basis functions on macro-domains. The higher order hierarchical basis functions [17-18] have been used to analyze the electromagnetic scattering from breaking waves [19].

In this paper, four types of higher order basis functions, that is, the hierarchical tangential vector basis functions [20, 35-36] with curvilinear triangle patch mesh, the higher order hierarchical basis functions [17-18] with curvilinear quadrilateral patch mesh, and the maximally orthogonalized higher order basis functions [21] with curvilinear quadrilateral patch mesh are used to analyze the electromagnetic scattering from the target and dielectric rough surface. The validities of these functions are compared. To the knowledge of the author, the higher order basis functions have not been used to analyze scattering from rough surfaces.

The remainder of this paper is organized as follows. In Section II, theory and formulations are discussed. Numerical results are presented and discussed in Section III. Section IV concludes this paper. The time factor $e^{j\omega t}$ is assumed and suppressed throughout this paper.

II. THEORY AND FORMULATION

A. Rough surface modeling and PMCHW integral equation

In practical cases, in order to eliminate the edge effects caused by truncation of the finite surface length, the tapered wave [16] is usually employed. Figure 1 shows the geometry of the proposed problem. The width of the tapered wave should be large enough to illuminate upon the surface. The incident electric and magnetic fields are $\mathbf{E}^{inc}$ and $\mathbf{H}^{inc}$. Region 1 and Region 2 are characterized by medium parameters (ε_1, μ_1) and (ε_2, μ_2) , respectively. The equivalent electric and magnetic surface currents **J(r)** and **M(r)** are impressed on the rough surface. For simplicity, the rough surface without object is considered here, the formulations for an object under a dielectric rough surface can be found in references [2, 23]. To obtain **J** and **M** , the PMCHW [5, 22] formulation enforces the continuity of the tangential electric and magnetic field components across *S*:

$$\mathbf{E}^{inc}(\mathbf{r})|_{\tan} = (L_1 + L_2)\mathbf{J}(\mathbf{r})|_{\tan} - (K_1 + K_2)\mathbf{M}(\mathbf{r})|_{\tan} . \quad (1)$$

$$\mathbf{H}^{inc}(\mathbf{r})|_{\tan} = (K_1 + K_2)\mathbf{J}(\mathbf{r})|_{\tan} + (\frac{1}{\eta_1^2}L_1 + \frac{1}{\eta_2^2}L_2)\mathbf{M}(\mathbf{r})|_{\tan} . \quad (2)$$

where η_1 and η_2 are the wave impedance of regions 1 and 2, respectively, and operators L_p and K_p (p=1,2) are defined by

$$L_p\mathbf{X}(\mathbf{r}) = \int_S ds'[\, j\omega\mu_p \mathbf{X}(\mathbf{r}') + \frac{j}{\omega\varepsilon_p}\nabla\nabla' \bullet \mathbf{X}(\mathbf{r}')]g_p(\mathbf{r},\mathbf{r}'), \quad (3)$$

$$K_p\mathbf{X}(\mathbf{r}) = \int_S ds'\mathbf{X}(\mathbf{r}') \times \nabla g_p(\mathbf{r},\mathbf{r}'), \quad (4)$$

where $g_p(\mathbf{r},\mathbf{r}')$ is the scalar Green's function

$$g_p(\mathbf{r},\mathbf{r}') = \frac{e^{-jk_p|\mathbf{r}-\mathbf{r}'|}}{4\pi|\mathbf{r}-\mathbf{r}'|}. \quad (5)$$

The solution of the PMCHW (equations (1-4)) obtains the electric and magnetic surface current densities **J** and **M** , which are required in the computation of the bistatic scattering coefficient (normalized RCS) [23].

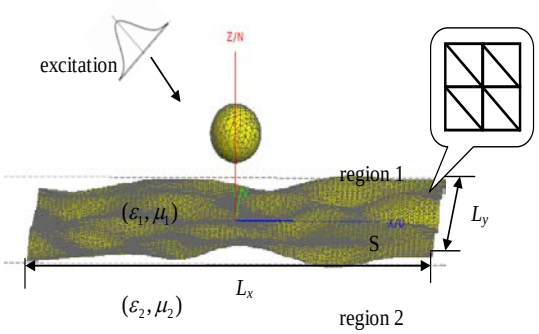

Fig. 1. Geometric model of EM scattering from the rough surface.

B. Higher order basis functions

In this paper, four types of higher order basis functions are used to analyze the electromagnetic scattering from the target and dielectric rough surface. For simplicity, the higher order hierarchical Legendre basis functions defined on the curvilinear quadrilateral surface are provided here. The specific forms of the hierarchical tangential vector basis functions on the curvilinear triangle patch [20, 35-36] and the maximally orthogonalized higher order basis functions on the curvilinear quadrilateral patch [21] can be found in the references.

The higher order hierarchical Legendre basis functions defined on the curvilinear quadrilateral surface [8-10] are

$$\mathbf{J}_S = J_S^u \mathbf{a}_u + J_S^v \mathbf{a}_v, \tag{6}$$

where $\mathbf{a}_u$ and $\mathbf{a}_v$ are the co-variant unitary vectors as $\mathbf{a}_u = \partial \mathbf{r} / \partial u$ and $\mathbf{a}_v = \partial \mathbf{r} / \partial v$. Without loss of generality, we consider only u-directed currents

$$J_S^u(u,v) = \frac{1}{\mathcal{J}_S(u,v)} \sum_{m=0}^{M^u} \sum_{n=0}^{N^v} a_{mn}^u \widetilde{C}_m \widetilde{P}_m(u) C_n P_n(v), \tag{7}$$

where $\mathcal{J}_S(u,v) = |\mathbf{a}_u \times \mathbf{a}_v|$ is the surface Jacobian, a_{mn}^u are unknown coefficients, and M^u and N^v are basis orders along the *u*-directed current flow direction and the transverse direction respectively. $P_n(v)$ are Legendre polynomials, and $\widetilde{P}_m(u)$ are modified Legendre polynomials, which can be defined as

$$\widetilde{P}_m(u) = \begin{cases} 1-u, & m=0 \\ 1+u, & m=1 \\ P_m(u) - P_{m-2}(u), & m \geq 2 \end{cases}, \tag{8}$$

where $\widetilde{C}_m$ and C_n are the scaling factors

$$\widetilde{C}_m = \begin{cases} \dfrac{\sqrt{3}}{4}, & m = 0,1 \\ \dfrac{1}{2}\sqrt{\dfrac{(2m-3)(2m+1)}{2m-1}}, & m \geq 2 \end{cases}. \tag{9}$$

$$C_n = \sqrt{n+\frac{1}{2}}. \tag{10}$$

C. Matrix vector product accelerated by the MLFMA

In the process of MLFMA, interactions between the elements are classified as near zone and far zone. The near-zone elements are calculated directly using the MoM, and the far-zone elements are calculated by using the MLFMA [24,32]. The Green's function in the FMM is

$$\frac{e^{-jk|\mathbf{r}+\mathbf{d}|}}{|\mathbf{r}+\mathbf{d}|} \approx -jk \sum_{l=\infty}^{L} (-1)^l (2l+1) j_l(kd) h_l^{(1)}(kr) P_l(\hat{d} \bullet \hat{r}), \tag{11}$$

where k is the wavenumber, j_l is a spherical Bessel function of the first kind, and P_l is a Legendre polynomial. $\mathbf{r}$ and $\mathbf{d}$ are two vectors with r and d being their amplitudes with $d < r$, and $\hat{r}$ and $\hat{d}$ being their unit vectors respectively. The number of modes L is usually chosen as $L = kd + \ln(\pi + kd)$. In the MLFMA, a matrix-vector product can be executed as follows: all basis functions in a group can be aggregated into an outgoing radiation pattern which is then translated to an incoming radiation pattern at the receiving group. The incoming radiation pattern is then disaggregated to the test functions. In order to accelerate the solving process, the FGMRES [25, 26] iterative solver is used.

III. NUMERICAL RESULTS

In this section several numerical results are presented for various models and basis functions, in which a Gaussian dielectric rough surface with the following Gaussian spectrum [27].

$$W(k_x, k_y) = \frac{l_x l_y h^2}{4\pi} e^{-\frac{l_x^2 k_x^2 + l_y^2 k_y^2}{4}}, \tag{12}$$

is used. Here, l_x and l_y are the correlation lengths in $x-$ and $y-$ directions respectively. h is the *rms* height of the rough surface.

The GMRES restart counts are set to 30 and the inner and outer restart counts of FGMRES are both 10. The stop precision for restarted GMRES is set to 1.E-3 and that for the inner and outer iteration in the FGMRES algorithm are 1.E-2 and 1.E-3 respectively. The method is implemented on a personal computer with Intel Dual-core CPU. The CPU and memory sizes are 2.99GHz and 3.24GB, respectively. In the numerical figures presented below, "0.5-t" denotes 0.5-order hierarchical tangential vector basis functions based on the curvilinear triangle mesh defined in [20]. "1.5-t" denotes 1.5-order hierarchical tangential vector basis functions based on the curvilinear triangle mesh defined in [20]. "1-q" denotes 1-order hierarchical Legendre basis functions based on curvilinear quadrilateral mesh, "2-q" denotes 2-order hierarchical Legendre basis functions based on the curvilinear quadrilateral mesh, and "2-m" denotes 2-order maximally orthogonalized higher order basis functions based on the curvilinear quadrilateral mesh. It should be noted that the expressions for 1-order maximally orthogonalized higher order basis functions are the same as those of 1-order hierarchical Legendre basis functions.

Firstly, the PMCHW computer code with different basis functions is compared with the shooting and bouncing rays method (SBR) [28]. The size of the rough surface is $16\lambda\times16\lambda$, with $h=0.04\lambda$ and $l_x=l_y=0.5\lambda$, where λ is the free-space wavelength. The dielectric constant is set to $\varepsilon_1=1,\varepsilon_2=5.4-j0.04$. The tapered wave is incident at the elevation angle $\theta_i=30^0$ and the azimuth angle $\varphi_i=0^0$, with tapering parameter $g=5.0\lambda$. Figure 2 is the bistatic RCS for HH polarization of these methods, which shows a reasonably good agreement.

In the second example the efficiency of the proposed method with different basis functions is evaluated. The size of the rough surface is $6\lambda\times6\lambda$, with $h=0.08\lambda$ and $l_x=l_y=1.5\lambda$. The dielectric constant is set to be $\varepsilon_1=1,\varepsilon_2=2.25$. The tapered wave is incident at the elevation angle $\theta_i=-30^0$ and the azimuth angle $\varphi_i=0^0$, with tapering parameter $g=3.0\lambda$. The size of the finest level blocks is $0.5\lambda\times0.5\lambda\times0.5\lambda$. Figure 3 is the bistatic RCS of different basis functions for HH polarization, which shows a good agreement. Table 1 gives comparisons of memory and time consumption, where "1.5-t [35,36]" denotes 1.5-order hierarchical tangential vector basis functions based on the curvilinear triangle mesh defined in [35, 36]. It should be noted that the expressions for 0.5-order hierarchical vector basis functions defined in [35, 36] are the same as those for 0.5-order hierarchical basis functions defined in [20].

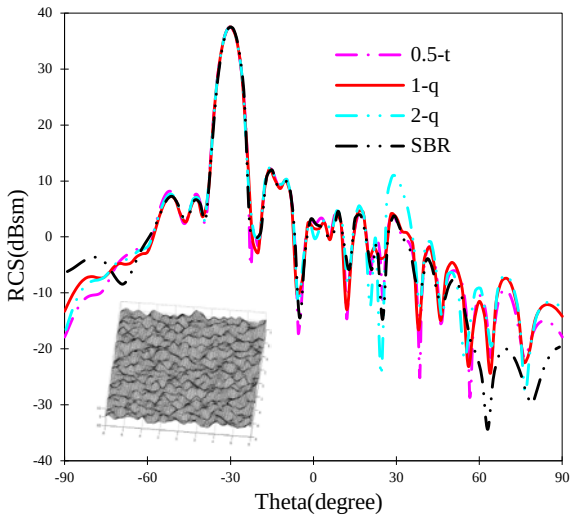

Fig. 2. Comparison of bistatic RCS of the dielectric rough surface for HH polarization.

The table shows that, the hierarchical Legendre basis functions based on the curvilinear quadrilateral mesh lead to a less total CPU time cost than the hierarchical tangential vector basis functions based on the curvilinear triangle mesh. For triangle cells, the basis functions defined in [35,36] lead to better condition numbers than the ones defined in [20], and results in less CPU time cost. Furthermore, the orthogonality of the maximally orthogonalzed higher order basis functions enable fast convergence of the iteration, which results in a minimum requirement of total CPU time.

In the third example, we consider a perfectly electrical conducting (PEC) sphere buried under a rough surface published in [23]. The size of the rough surface is $8\lambda\times8\lambda$, with $h=0.02\lambda$ and

$l_x = l_y = 0.5\lambda$. The tapering parameter is $g = 2.0\lambda$. The dielectric constant is set to $\varepsilon_1 = 1, \varepsilon_2 = 2 - j0.2$. A sphere of radius $a = 0.3\lambda$ is buried under the rough surface at a depth of $d = 0.6\lambda$.

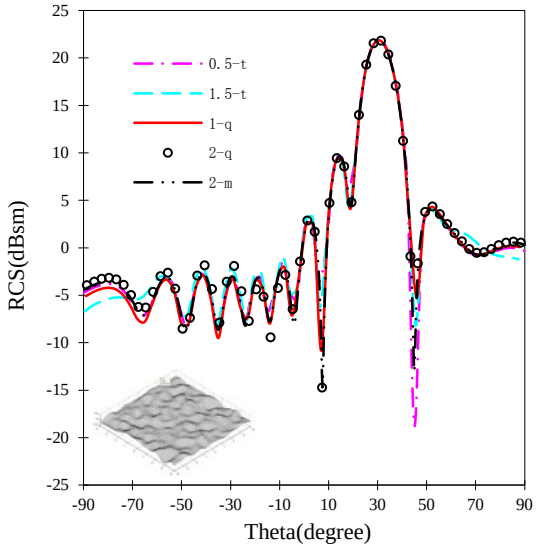

Fig. 3. Bistatic RCS of the dielectric rough surface for HH polarization.

Table 1: Cost comparison among different basis functions

Basis functions	Mesh size (λ)	Total unknowns	Near field filling time (sec.)
0.5-t	0.1	21,360	105
1.5-t	0.2	17,760	56
1.5-t-[35][36]	0.2	17,760	54
1-q	0.1	14,160	151
2-q	0.2	14,160	33
2-m	0.2	14,160	33

Basis functions	Iteration Number	Total time(sec.)	Memory cost(MB)
0.5-t	19	209	211
1.5-t	44	253	158
1.5-t-[35][36]	27	181	158
1-q	13	197	112
2-q	31	138	112
2-m	18	94	112

Figure 4 is the normalized RCS of different basis functions for HH polarization. The difference between the method presented in this paper and the references for some observation angles can be interpreted as that the rough surface used in this example is different from that in the references, which is a Gaussian stationary stochastic process. Table 2 gives comparisons of memory and time consumption. The table shows that the fill time of near field for "1.5-t" is smaller than that for "0.5-t". However, due to the truncation of the dielectric rough surface, the interaction between the object and the rough surface, and the individual characteristics of the higher order basis functions, the condition numbers of the system become higher with the basis order increase. Consequently, the iteration time of the "1.5-t" is longer than that of "0.5-t", which also applies to the Legendre basis functions. However, the maximally orthogonalzed higher order basis functions, have a smaller iteration steps compared to "1.5-t" and "2-q", which results in a minimum requirement of total CPU time.

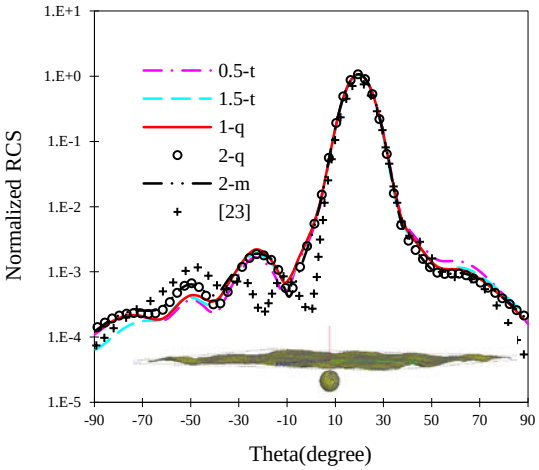

Fig. 4. Normalized RCS for a PEC sphere buried under a rough surface.

Finally, we consider a PEC sphere above a rough surface. The size of the rough surface is $8\lambda \times 8\lambda$, with $h = 0.02\lambda$ and $l_x = l_y = 0.5\lambda$. The tapering parameter is $g = 3.0\lambda$. The dielectric constant is set to $\varepsilon_1 = 1, \varepsilon_2 = 2 - j0.2$. A sphere of radius $a = 0.3\lambda$ is above the rough surface at a height of $d = 0.6\lambda$. Figure 5 is the bistatic RCS of different basis functions for HH polarization, and Table 3 gives comparisons on memory and time

consumption. Different from the third example, the CPU time cost of the three types basis functions decreases with the basis order increase, and the maximally orthogonalized higher order basis functions have a minimum requirement in total CPU time.

Table 2: Cost comparison among different basis functions

Basis functions	Mesh size (λ)	Total unknowns	Near field filling time (sec.)
0.5-t	0.1	38,404	276
1.5-t	0.2	32,000	110
1-q	0.1	25,592	298
2-q	0.2	25,472	64
2-m	0.2	25,472	64

Basis functions	Iteration number	Iteration time(sec.)	Total time(sec.)	Memory cost(MB)
0.5-t	17	188	487	393
1.5-t	57	506	631	296
1-q	12	88	493	211
2-q	87	577	663	210
2-m	18	124	210	210

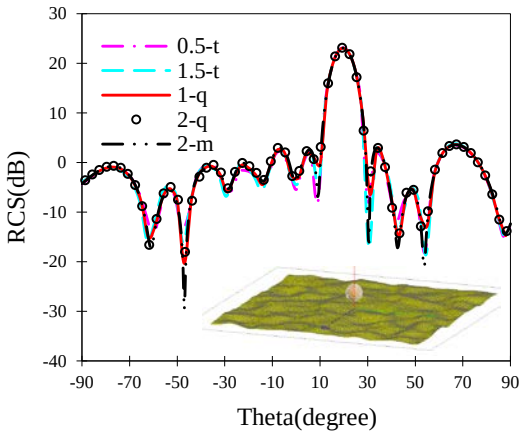

Fig. 5. Bistatic RCS for a PEC sphere above a rough surface.

Table 3: Cost comparison among different basis functions

Basis functions	Mesh size(λ)	Total unknowns	Near field filling time (sec.)
0.5-t	0.1	38,401	415
1.5-t	0.2	32,000	160
1-q	0.1	25,592	439
2-q	0.2	25,472	89
2-m	0.2	25,472	89

Basis functions	Iteration Number	Iteration time(sec.)	Total time(sec.)	Memory cost(MB)
0.5-t	16	191	606	559
1.5-t	47	437	597	415
1-q	11	74	513	292
2-q	28	178	267	289
2-m	15	98	187	289

IV. CONCLUSION

Numerical simulation of the combined target and rough surface model is complicated by the truncation of the dielectric rough surface and the interaction between the object and rough surface. In this paper, four types of higher order basis functions are used to analyze the EM scattering from the target and dielectric rough surface. Numerical simulation shows a reasonably good agreement with the SBR and references. For the target above the rough surface or only the rough surface case, the hierarchical Legendre basis functions based on the curvilinear quadrilateral mesh are more efficient than the hierarchical tangential vector basis functions based on the curvilinear triangle mesh in CPU time with the increase of the basis order. The maximally orthogonalized higher order basis functions show an excellent efficiency in dealing with all of the three cases.

ACKNOWLEDGMENT

The authors would like to thank the support of Major State Basic Research Development Program of China (973 Program: 2009CB320201), Natural Science Foundation of 61001009, and Jiangsu Natural Science Foundation of BK2008048.

REFERENCES

[1] J. T. Johnson, "A Numerical Study of Scattering from an Object Above a Rough Surface," *IEEE Trans. Antennas Propag.*, vol. 50, no. 10, pp. 1361-1367, Oct. 2002.

[2] M. El-Shenawee, C. Rappaport, E. L. Miller, and M. B. Silevitch, "Three-Dimensional Subsurface Analysis of Electromagnetic Scattering from Penetrable/PEC Objects Buried under Rough Surfaces: Use of the Steepest Descent Fast Multipole Method." *IEEE Trans. Geosci. Remote Sens.*, vol. 39, no. 6, pp. 1174-1182, June 2001.

[3] H. Ye and Y.-Q. Jin, "A Hybrid Analytic-Numerical Algorithm of Scattering from an Object above a Rough Surface," *IEEE Trans. Geosci. Remote Sens.*, vol. 45, no. 5, pp. 1174-1180, May 2007.

[4] F.-S Deng, S.-Y. He, H.-T. Chen, W.-D. Hu, W.-X Yu, and G.-Q. Zhu, "Numerical Simulation of Vector Wave Scattering from the Target and Rough Surface Composite Model with 3-D Multilevel UV Method," *IEEE Trans. Antennas Propag.*, vol. 58, no. 5, pp. 1625–1634, May 2010.

[5] V. Jandhyala, B. Shanker, E. Michielssen, and W. C. Chew, "Fast Algorithm for the Analysis of Scattering by Dielectric Rough Surfaces," *J. Opt. Soc. Am. A*, vol. 15, no. 7, pp. 1877-1885, July 1998.

[6] V. Jandhyala, E. Michielssen, S. Balasubramaniam, and W. C. Chew, "A Combined Steepest Descent-Fast Multipole Algorithm for the Fast Analysis of Three-Dimensional Scattering by Rough Surfaces," *IEEE Trans. Geosci. Remote Sens.*, vol. 36, no. 3, pp. 738-748, May 1998.

[7] A. Yagbasan, C. A. Tunc, V. B. Ertürk, A. Altintas, and R. Mittra, "Characteristic Basis Function Method for Solving Electromagnetic Scattering Problems over Rough Terrain Profiles," *IEEE Trans. Antennas Propag.*, vol. 58, no. 5, pp. 1579–1589, May 2010.

[8] C.-H. Kuo and M. Moghaddam, "Electromagnetic Scattering from a Buried Cylinder in Layered Media with Rough Interfaces," *IEEE Trans. Antennas Propag.*, vol. 54, no. 8, pp. 2392-2401, August 2006.

[9] B. Liu, Z. Li, and Y. Du, "A Fast Numerical Method for Electromagnetic Scattering from Dielectric Rough Surfaces," *IEEE Trans. Antennas Propag.*, vol. 59, no. 1, pp. 180-188, January 2011.

[10] A. Tabatabaeenejad and M. Moghaddam, "Bistatic Scattering from Three-Dimensional Layered Rough Surfaces," *IEEE Trans. Geosci. Remote Sens.*, vol. 44, no. 8, pp. 2102-2114, 2006.

[11] A. G. Voronovich, "Small-Slope Approximation for Electromagnetic Wave Scattering at a Rough Interface of Two Dielectric Half-Spaces," *Waves in Random Media*, vol. 4, iss. 3, pp. 337-367, 1994.

[12] M. R. Pino, R. J. Burkholder, and F. Obelleiro, "Spectral Acceleration of the Generalized Forward-Backward Method," *IEEE Trans. Antennas Propag.*, vol. 50, no. 6, pp. 785-797, June 2002.

[13] P. Liu and Y. Q. Jin, "Numerical Simulation of Bistatic Scattering from a Target at Low Altitude above Rough Sea Surface under an EM-Wave Incidence at Low Grazing Angle by Using the Finite Element Method," *IEEE Trans. Antennas Propag.*, vol. 52, no. 5, pp. 1205-1210, May 2004.

[14] L. Kuang and Y. Q. Jin, "Bistatic Scattering from a Three-Dimensional Object over a Randomly Rough Surface using the FDTD Algorithm," *IEEE Trans. Antennas Propag.*, vol. 55, no. 8, pp. 2302–2312, August 2007.

[15] J. T. Johnson, L. Tsang, R. T. Shin, K. Pak, C. H. Chan, A. Ishimaru, and Y. Kuga, "Backscattering Enhancement of Electromagnetic Waves from Two-Dimensional Perfectly Conducting Random Rough Surfaces–a Comparison of Monte Carlo Simulations with Experimental Data," *IEEE Trans. Antennas Propag.*, vol. 44, pp. 748–756, May 1996.

[16] L. Tsang, J. A. Kang, F. H. Ding, and C. D. Ao, *Scattering of Electro Magnetic Wave; Numerical Simulation*, New York: Wiley, 2001.

[17] E. Jørgensen, J. L. Volakis, P. Meincke, and O. Breinbjerg, "Higher Order Hierarchical Legendre Basis Functions for Electromagnetic Modeling," *IEEE Trans. Antennas Propag.*, vol. 52, no. 11, pp. 2985-2995, 2004.

[18] E. Jørgensen, O. S. Kim, P. Meincke, and O. Breinbjerg, "Higher Order Hierarchical Discretization Scheme for Surface Integral Equations for Layered Media," *IEEE Trans. Geosci. Remote Sens.*, vol. 42, no. 4, pp. 346-352, 2004.

[19] W. Yang, Z. Zhao, C. Qi, and Z. Nie, "Electromagnetic Modeling of Breaking Waves at Low Grazing Angles with Adaptive Higher Order Hierarchical Legendre Basis Functions." *IEEE Trans. Geosci. Remote Sens.*, vol. 49, no. 1, pp. 346-352, 2011.

[20] L. S. Andersen and J. L. Volakis, "Hierarchical Tangential Vector Finite Elements for Tetrahedra," *IEEE Microwave and Guided Wave Letters*, vol. 8 no. 3 pp. 127-129, March 1998.

[21] D. S. Sumic and B. M. Kolundzija, "Efficient Iterative Solution of Surface Integral Equation Based on Maximally Orthogonalized Higher

Order Basis Functions," *Proc. IEEE Antennas Propag. Society Int. Sym.*, session 116, 2005.

[22] A. J. Poggio and E. K. Miller, *Integral Equation Solutions of Three-Dimensional Scattering Problems*, *Computer Techniques for Electromagnetics*, pp. 159-264, Pergamon Press, Oxford and New York, 1973.

[23] G. Zhang and L. Tsang, "Angular Correlation Function and Scattering Coefficient of Electromagnetic Waves Scattered by a Buried Object under a Two-Dimensional Rough Surface," *J. Opt. Soc. Am. A*, vol. 15, no. 12, pp. 2995-3002, Dec. 1998.

[24] J. Song, C. C. Lu, and W. C. Chew, "Multilevel Fast Multipole Algorithm for Electromagnetic Scattering by Large Complex Objects," *IEEE Trans. Antennas Propag*., vol. 45, no. 10, pp. 1488-1493, Oct. 1997.

[25] Y. Saad and M. H. Schultz, "GMRES: A Generalized Minimal Residual Algorithm for Solving Nonsymmetric Linear Systems," *SIAM J. Sci. Statist. Comput.*, vol. 7, pp. 856-869, July 1986.

[26] Y. Saad., "A Flexible Inner-Outer Preconditioned GMRES Algorithm," *SIAM J. Sci. Statist. Comput.*, vol. 14, pp. 461-469, 1993.

[27] K. Pak, L. Tsang, C. H. Chan, and J. T. Johnson, "Back Scattering Enhancement of Electromagnetic Waves from Two-Dimensional Perfectly Conducting Random Rough Surface Based on Monte Carlo Simulations," *J. Opt. Soc. Amer. A, Opt. ImageSci.*, vol. 12, no. 11, pp. 2491–2499, Nov. 1995.

[28] H. Ling, R. C. Chou, and S. W. Lee, "Shooting and Bouncing Rays: Calculating the RCS of an Arbitrarily Shaped Cavity," *IEEE Trans. Antennas Propag.*, vol. 37, no. 2, pp. 194-205, Feb. 1989.

[29] R. Araneo and S. Barmada, "Advanced Image Processing Techniques for the Discrimination of Buried Objects," *Applied Computational Electromagnetics Society (ACES) Journal*, vol. 26, no. 5, pp. 437-446, May 2011.

[30] J. Li, L. X. Guo, and H. Zeng, "FDTD Investigation on Electromagnetic Scattering from Two-Dimensional Layered Rough Surfaces," *Applied Computational Electromagnetics Society (ACES) Journal*, vol. 25, no. 5, pp. 450-457, May 2010.

[31] M. El-Shenawee and C. M. Rappaport, "Monte Carlo Simulations for Clutter Statistics in Minefields: AP-Mine-Like-Target Buried Near a Dielectric Object beneath 2-D Random Rough Ground Surfaces," *IEEE Trans. Geosci. Remote Sens.*, vol. 40, no. 6, pp. 1416-1426, 2002.

[32] Z. Jiang, Y. Xu, R. S. Chen, Z.H. Fan, and D. Z. Ding, "Efficient Matrix Filling of Multilevel Simply Sparse Method Via Multilevel Fast Multipole Algorithm," *Radio Science*, 2011.

[33] C.-H. Kuo and M. Moghaddam, "Scattering from Multilayer Rough Surfaces Based on the Extended Boundary Condition Method and Truncated Singular Value Decomposition," *IEEE Trans. Antennas Propag.*, vol. 54, no. 10, pp. 2917-2929, Oct. 2006.

[34] P. Ingelström, "A New Set of H (Curl)-Conforming Hierarchical Basis Functions for Tetrahedral Meshes," *IEEE Transactions on Microwave Theory and Techniques*, vol. 54, no. 1, pp. 106-114, Jan. 2006.

[35] R. D. Graglia, A. F. Peterson, and F. P. Andriulli, "Curl-Conforming Hierarchical Vector Bases for Triangles and Tetrahedral," *IEEE Trans. Antennas Propag.*, vol. 59, no. 3, pp. 950-959, Mar. 2011.

[36] L. P. Zha, Y. Q. Hu, and T. Su, "Efficient Surface Integral Equation using Hierarchical Vector Bases for Complex EM Scattering Problems," *IEEE Trans. Antennas Propag.*, vol. 60, no. 2, pp. 952-957, Feb. 2012.

[37] A. F. Peterson and R. D. Graglia, "Scale Factors and Matrix Conditioning Associated with Triangular-Cell Hierarchical Vector Basis Functions," *IEEE Antennas and Wireless Propagation Letters*, vol. 9, pp. 40-43, 2010.

[38] A. F. Peterson and R. D. Graglia, "Evaluation of Hierarchical Vector Basis Functions for Quadrilateral Cells," *IEEE Trans. Magnetics*, vol. 47, pp. 1190-1193, May 2011.

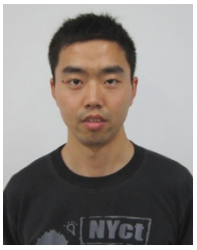

Yuyuan An was born in Sichuan province, China, in 1986. He received the B.S. degree from Nanjing University of Science and Technology (NJUST) in 2009, and is currently working toward the Ph.D. degree at NJUST. His current research interests include computational electromagnetics, antennas, electromagnetic scattering and propagation, and electromagnetic modeling of microwave integrated circuits.

Rushan Chen was born in Jiangsu, P. R. China. He received his B.Sc. and M.Sc. degrees from the Dept. of Radio Engineering, Southeast University, in 1987 and in 1990, respectively, and his Ph.D. from the Dept. of Electronic Engineering, City University of Hong Kong in 2001. He joined the Dept. of Electrical Engineering, Nanjing University of Science & Technology (NJUST), where he became a Teaching Assistant in 1990 and a

Lecturer in 1992. He has authored or co-authored more than 200 papers, including over 140 papers in international journals. He is the recipient of the Foundation for China Distinguished Young Investigators presented by the National Science Foundation (NSF) of China in 2003. In 2008, he became a Chang-Jiang Professor under the Cheung Kong Scholar Program awarded by the Ministry of Education, China. His research interests mainly include microwave/millimeter-wave systems, measurements, antenna, RF-integrated circuits, and computational electromagnetics.

Pingping Xu was born in Jiangsu province, China. She received the B.S. degree from Huaiyin Normal College in 2009, and is currently working toward the M.S. degree at NJUST. Her current research interests include computational electromagnetics, antennas, electromagnetic scattering and propagation, and electromagnetic modeling of microwave integrated circuits.

Zhiwei Liu was born in Nanchang, Jiangxi, China in 1982. He received B.S. degree in Computer Science from Nanjing University of Science and Technology in 2003, M.S. degree in Nanjing Institute of Electronics and Technology in 2006, and Ph.D. degree in Nanjing University of Science and Technology in 2011, respectively. He was with the Department of Electrical and Computer Engineering, Iowa State University, as a visiting scholar in 2009. He is currently working at School of Information Engineering, East China Jiaotong University. His research interests focus on the theory of electromagnetic scattering and inverse scattering.

Liping Zha was born in Anhui Province, China, in 1987. She received the B.S. degree in Electronic Information Engineering from Anhui University of Architecture, China, in 2008, and is currently working toward the Ph.D. degree at Nanjing University of Science and Technology (NJUST), Nanjing, China. Her current research interests include computational electromagnetics, electromagnetic modeling of scattering problems, wave scattering and propagation from random media, and numerical techniques for electrically large objects.